Evaluation of Dose and Safety of AAV7m8 and AAV8BP2 in the Non-Human Primate Retina

Pavitra S. Ramachandran, Vivian Lee, Zhangyong Wei, Ji Yun Song, Giulia Casal, Therese Cronin, Keirnan Willett, Rachel Huckfeldt, Jessica I.W. Morgan, Tomas S. Aleman, Albert M. Maguire, and Jean Bennett*

Center for Advanced Retinal and Ocular Therapeutics (CAROT) and F.M. Kirby Center for Molecular Ophthalmology, Scheie Eye Institute, University of Pennsylvania Perelman School of Medicine, Philadelphia, Pennsylvania.

Within the next decade, we will see many gene therapy clinical trials for eye diseases, which may lead to treatments for thousands of visually impaired people around the world. To target retinal diseases that affect specific cell types, several recombinant adeno-associated virus (AAV) serotypes have been generated and used successfully in preclinical mouse studies. Because there are numerous anatomic and physiologic differences between the eyes of mice and "men" and because surgical delivery approaches and immunologic responses also differ between these species, this study evaluated the transduction characteristics of two promising new serotypes, AAV7m8 and AAV8BP2, in the retinas of animals that are most similar to those of humans: non-human primates (NHPs). We report that while AAV7m8 efficiently targets a variety of cell types by subretinal injection in NHPs, transduction after intravitreal delivery was mostly restricted to the inner retina at lower doses that did not induce an immune response. AAV8BP2 targets the cone photoreceptors efficiently but bipolar cells inefficiently by subretinal injection. Additionally, transduction by both serotypes in the anterior chamber of the eye and the optic pathway of the brain was observed post-intravitreal delivery. Finally, we assessed immunogenicity, keeping in mind that these AAV capsids may be used in future clinical trials. We found that AAV8BP2 had a better safety profile compared with AAV7m8, even at the highest doses administered. These studies underscore the differences in AAV transduction between mice and primates, highlighting the importance of careful evaluation of therapeutic vectors in NHPs prior to moving to clinical trials.

Keywords: retina, AAV, gene therapy, non-human primate, animal models

INTRODUCTION

IN RECENT YEARS, CLINICAL TRIALS have demonstrated a high degree of safety with respect to delivery of recombinant adeno-associated virus serotype 2 (AAV2) vectors to the eye. Wildtype AAVs are non-pathogenic, single stranded DNA viruses that require a helper virus such as adenovirus to replicate. Recombinant AAV vectors do not replicate, even with the addition of helper viruses, and have been used for more than two decades to deliver transgenes *in vivo* stably and efficiently. The eye is well suited for gene therapy for many reasons: low doses of AAV are sufficient to transduce the target cells, there is a great deal of progress in understanding the pathogenetic mechanisms of disease, the tissue can be directly visualized, surgical approaches for gene delivery are well developed, there are non-invasive tests for safety and efficacy studies, and there are tissue layers that lack a direct blood supply—a fact that contributes to favorable immunologic properties. More than a dozen human clinical trials have been carried out for ocular diseases using AAV2. The first gene therapy study that has proceeded through Phase III (efficacy) clinical trials in the human eye used AAV serotype 2 to deliver the wildtype *RPE65* cDNA into the retinal pigment epithelial (RPE) cells of Leber's congenital amaurosis type 2 (LCA2)

*Correspondence: Jean Bennett, Center for Advanced Retinal and Ocular Therapeutics (CAROT), 309C Stellar-Chance Labs; 422 Curie Blvd, Philadelphia, PA 19104. E-mail: jebennet@mail.med.upenn.edu

DOI: 10.1089/hum.2016.111

patients.[1] This study incorporated bilateral injections after prior studies showed that readministration of AAV to the contralateral eye was safe as well as efficacious.[2,3]

Since the identification of the archetypical AAV2, a number of other naturally occurring AAV serotypes have been isolated from humans or macaques, and many novel AAVs have been engineered in order to enhance transduction properties,[4,5] including efficiency of targeting particular cell types, onset of expression, and the ability to penetrate across tissue planes. While most AAV serotypes transduce RPE cells after subretinal injection, not all of them target rod or cone photoreceptors, or other ocular cell types efficiently. Further, the route of delivery can also affect tropism due to physiological barriers. In the retina for instance, intravitreal injections (IVI) of AAV2 result in the transduction of the innermost retinal ganglion cells and not the photoreceptors in the outer retina due in part to the presence of the inner limiting membrane.[6,7] In contrast, subretinal injections of AAV2 result in transduction of the RPE and photoreceptors in both small and large animal models.[8,9] Subretinal injections require specialized training in vitreo-retinal surgery, use of an operating room, and immobilization of the eye (usually through general anesthesia), and they are more technically challenging and carry the risk of retinal tears, unresolved detachments, and macular hole. It is thus attractive to consider AAV delivery by IVI. IVI is less invasive and is performed routinely in humans for delivery of other drugs as an office procedure. The idea of generating novel AAV capsids that could penetrate the retina and target photoreceptors after intravitreal delivery thus promised to revolutionize retinal gene therapy. The first such capsid generated by *in vivo* directed evolution in the mouse retina is AAV7m8. Dalkara *et al.* reported that IVI of AAV7m8 resulted in efficient pan-retinal photoreceptor and RPE transduction in the mouse.[10] They also showed that in the non-human primate (NHP) retina, IVI of high dose (5E + 12 vector genomes [vg]) AAV7m8 resulted in transduction of foveal photoreceptors. In addition, extrafoveal photoreceptors were transduced. However, the authors reported toxicity in an NHP injected with the high titer of AAV7m8, and had to terminate the study. Thus, a study of safety and efficiency of transduction using lower doses is warranted if this capsid is to be used in primates, including humans. It also needs to be determined if at lower titers, this capsid does indeed target the photoreceptors from the vitreous aspect.

Cells within the retina that have been challenging to transduce with AAV are the ON-bipolar cells. These cells relay information from the photoreceptors to the ganglion cells. The ON-bipolar cells are a target for retinal optogenetic therapies and other gene augmentation approaches.[11–14] Work from our group generated a novel capsid called AAV8BP2 by *in vivo* directed evolution. AAV8BP2 targets the ON-bipolar cells effectively by subretinal injections in the mouse.[15] AAV8BP2-mediated optogenetic delivery to the ON-bipolar cells resulted in a restoration of retinal ganglion cell responses in retinal degeneration mice.[15]

While these two novel AAVs have shown exciting promise in mice, species-specific differences can result in different patterns of tropism, as has been shown before in the retina, as well as in other organ systems.[16,17] Thus, while one particular AAV serotype-driven gene therapy may result in rescue of a mouse phenotype, it may not have the same effect in a large animal (or human) retina. To address this concern, this study evaluated two novel AAV capsids, AAV7m8 and AAV8BP2, in the (normal-sighted) NHP model. The goals were to characterize cellular transduction patterns and to assess safety after IVI versus subretinal injection of a range of doses of the AAVs in the primate eye. In addition to evaluating the posterior pole (retina, choroid, optic nerve) of the eye, transduction of cells of the anterior segment (ciliary body, lens, iris, cornea) were characterized, since intravitreal delivery would likely result in exposure to these structures.

Here, expression of the reporter gene encoding enhanced green fluorescent protein (eGFP) is used, driven by a constitutive promoter to present a comprehensive dose-ranging study of AAV7m8 and AAV8BP2 in the NHP eye, and the cellular specificity of transduction after IVI or subretinal injection is compared and contrasted. The immunologic and histopathologic data from these eyes/animals are also presented. Together, the data provide suggestions pertaining to potential applications, dosing, and limitations of these two vectors in therapeutic paradigms. Finally, the data reveal that for evolutionary design to be used to generate vectors with properties relevant to human application, it may be important to carry out the procedural steps using target cells more closely related to those of *Homo sapiens*. For human application, generation of novel AAVs by directed evolution using retinal explant cultures derived from NHPs or even from postmortem human samples may be optimal.

We established that AAV7m8 targets photoreceptors (in addition to other cell types) of the retina

by subretinal injections at a range of doses, but is only able to transduce photoreceptors at the highest dose tested by IVI. We showed that AAV8BP2 targets the photoreceptors by subretinal delivery and ganglion cells after delivery from the vitreous aspect. However, the ON-bipolar cells are poorly transduced by either route of delivery of AAV8BP2, indicating either species-specific differences with respect to this capsid or perhaps a mechanical barrier to transduction (e.g., photoreceptor outer segments or the outer limiting membrane) in the wildtype NHP retina. We show that in a retinal degeneration dog model (where the photoreceptors are compromised), AAV8BP2 is able to transduce the ON-bipolar cells due to the lack of a mechanical barrier. Transduction of anterior segment structures after delivery of either AAV7m8 or AAV8BP2 by IVI was also observed. In addition, transduction into the visual pathway of the brain with both capsids was evaluated. Inflammation was assessed, and neutralizing antibody titers were determined to shed light on the safety of these serotypes at the different doses delivered. Thus, this study was performed with the hope that these results will be predictive of the safety and expression of these AAVs in human patients.

MATERIALS AND METHODS

AAV vectors and injections

The AAV proviral vector consisted of the CMV enhancer/CBA promoter (derived from Invivogen pDRIVE CAG plasmid), the cDNA encoding enhanced GFP (eGFP) protein, and the bovine growth hormone (bGH) polyadenylation signal. The AAVs were generated according to previously described methods[9] and purified by CsCl at the Children's Hospital of Philadelphia (CHOP) Vector Core, Philadelphia, Pennsylvania. The AAV7m8 capsid plasmid was a kind gift from Dr. Flannery. Vectors were stored with 0.001% Pluronic F-68 at –80°C until just before use, and then were diluted to the appropriate concentration.

Animals

The studies were performed in compliance with federal and institutional mandates. Mice were maintained under a 12 h light/dark cycle. Adult normal-sighted cynomolgous macaques were housed and cared for at the animal facility at the CHOP. The macaques had been used previously for a pharmacological study of an orally administered drug irrelevant to retinal/neuronal/immunologic function. The Crd1 (retinal degeneration) dog had been provided generously by Dr. G. Acland of the UPenn Retinal Disease Studies (RDS) facility and housed in the UPenn medical school facility. Optical coherence tomography (OCT) was carried out with a Heidelberg Spectralis.

IVI and subretinal injections in NHPs. IVI or subretinal injections were carried out under coaxial illumination through the operating microscope and after administering anesthesia with ketamine and dexmedetomidine. Injections were carried out after performing an anterior chamber fluid paracentesis to make space for the injected volume. Injections were performed using a Dutch Ophthalmic retractable TPA injection 41-gauge cannula and a 23-gauge valved entry system (Dutch Ophthalmic USA). Subretinal injections targeted the superior region of the macula, which in some cases also included the fovea (see Tables 1 and 2). The AAVs were injected at doses ranging from 1E + 9 vg to 1E + 12 vg so as to evaluate a potential dose response and/or dose-limiting toxicity. Atipamezole was administered at the end of the procedure to reverse anesthesia. The 23-gauge port wound was closed with 8-0 vicryl suture. Immediately after injection, the retinas were examined by indirect ophthalmoscopy to document the location of injection and whether there were any surgical complications. Kenalog (0.1 mL of 40 mg/mL) was injected sub-conjunctivally to minimize inflammation due to the surgical procedure before the animal had awoken, and the cornea was dressed with steroid/

Table 1. *Intraocular injection details*

AAV serotype	*NHP ID*	*Right versus left eye*	*Dose (vg)*	*Volume injection (μL)*	*Other*
Intravitreal					
AAV8b	05D 370	Left	1E + 09	150	
	05C 028	Left	1E + 10	150	
	9986	Right	1E + 11	150	
	9986	Left	1E + 12	150	
AAV7m8	05C 068	Right	1E + 08	150	
	07D 179	Left	1E + 09	150	
	05C 028	Right	1E + 10	150	
	5098	Right	1E + 11	150	
	9820	Right	1E + 12	150	Injection over fovea
	9820	Left	6.67E + 11	100	
Subretinal					
AAV8b	04C094	Right	1.0E + 10	150	
	04C 076	Left	1.5E + 11	150	
	99-09	Right	1E + 12	150	
	99-09	Left	1E + 12	150	SR (50)/IV (100)
AAV7m8	O4C094	Left	1.0E + 10	150	
	9817	Right	5.33E + 10	80	
	04C 076	Right	1.5E + 11	150	Focal hemorrhage at retinotomy site
	5285	Right	1E + 12	150	

Table 2. *Tropism of AAV7M8 and AAV8BP2 at different titers*

AAV serotype	*Delivery route*	*Dose (vg)*	*RPE*	*PR*	*INL*	*RGC*	*MC*	*ON*	*AS*
AAV8b	IVI	1E + 09	–	–	–	–	–	–	–
	IVI	1E + 10	–	–	–	–	–	–	–
	IVI	1E + 11	–	–	+	+	–	+	–
	IVI	1E + 12	–	–	+	+	–	+	+
	SR	1.0E + 10	+	+	–	+	–	+	–
	SR	1.5E + 11	+	+	+	+	–	+	–
	SR	1E + 12	+	+	+	+	–	+	–
AAV7m8	IVI	1E + 08	–	–	–	–	–	–	
	IVI	1E + 09	–	–	–	–	–	–	–
	IVI	1E + 10	–	–	+	+	+	+	+
	IVI	1E + 11	–	–	+	+	+	+	+
	IVI	6.67E + 11	–	–	+	+	+	+	+
	IVI	1E + 12	+	+	+	+	+	+	+
	SR	1.0E + 10	+	+	–	+	–	+	–
	SR	5.33E + 10	+	+	+	+	–	+	–
	SR	1.5E + 11	+	+	+	+	–	+	–
	SR	1E + 12	+	+	+	+	–	+	–

150 μL of adeno-associated virus (AAV) at the specified titer was delivered by subretinal (SR) or intravitreal injection (IVI). Positive eGFP expression apparent in tissue sections is indicated as by a "+" and no expression by a "–" in the cell types: RPE, retinal pigment epithelium; PR, photoreceptors; INL, inner nuclear layer; RGC, retinal ganglion cells; MC, Muller cells; ON, optic nerve; AS, anterior segment.

antibiotic (prednisolone 1%/gentamycin 1%) ointment. Animals were examined by indirect ophthalmoscopy on days 0, 3, and 30.

Subretinal injections in the mouse. Mice (aged >1 month) were anesthetized with ketamine/xylazine, and AAV7m8-CMV/CBA-eGFP at a dose of $\sim$2E + 9 vg was injected using a trans-choroidal approach in 2 μL of Dulbecco's phosphate-buffered saline (PBS).

Tissue harvesting and histology

NHPs were euthanized 1 month post injection. Upon euthanasia, serum, anterior chamber fluid, and vitreous samples were obtained, and the eyes and brain were removed and fixed in 4% paraformaldehyde. The anterior segment of the eyes was dissected from the posterior eyecup and placed in PBS containing 30% sucrose overnight at 4°C. The posterior pole, including the region exposed to AAV during subretinal injection, the fovea, and the optic disc, was isolated and was cryoprotected in 30% sucrose/PBS. Mouse eyes were also harvested 1 month post injection and cryopreserved in a similar manner for sectioning. Tissue was embedded in optimal cutting temperature media (Fisher Scientific Co.) and cryosectioned (12 μm) on the Leica CM1850 cryostat (Leica Microsystems).

Sections were evaluated for direct eGFP fluorescence. Immunofluorescent detection of eGFP was used in cases where eGFP was undetectable by direct fluorescence to confirm the absence of eGFP (AAV7m8 at 1E + 8 and 1E + 9 vg, and AAV8b at 1E + 9 and 1E + 10 vg tissue sections). For immunohistochemistry (IHC), the eye sections were blocked with 5% goat serum in 0.1% PBST (Triton X-100) for 1 h at room temperature. Anti-eGFP primary antibodies (Molecular probes A11122; Life Technologies) diluted at 1:200 in blocking solution were applied to the sections overnight. Anti-GFAP antibody (z0334; Dako) was used at 1:400, and the biotinylated PNA antibody (1075; Vector Labs) at 1:200. Anti-Goα (MAB3073; EMD Millipore) was used at 1:200, anti-CHAT (AB144P; Millipore) at 1:100, and anti-CHX10 (sc-365519; Santa Cruz) at 1:200 in blocking solution overnight. Secondary antibodies 1:200 Alexa fluor (Life Technologies) and 1:250 Streptavidin conjugated Cy3 (434315; Invitrogen) were applied for 1 h at room temperature, washed in PBS, and mounted with DAPI (4′,6-diamidino-2-phenylindole) in Fluoromount-G (Southern Biotech). All slides were then viewed on a confocal laser-scanning microscope (Olympus Fluoview 1000). Hematoxylin and eosin (H&E) staining was performed on retinal sections adjacent to those in which immunofluorescence had been performed using standard procedures.[9,18] Images were then collected using AxioVision software on the Nikon Eclipse 80i microscope.

Brain histology

Post fixation in 10% formalin, the brain was cut into blocks and sectioned on the Leica sliding microtome. Free-floating sections (50 μm) were sectioned and stored in cryopreservative solution at –20°C until analyzed. Nissl staining was performed on brain sections by standard methods. All

sections were mounted onto Superfrost Plus slides (Brain Research Labs) and mounted with Cytoseal 60 (Thermo Scientific). Images were then collected using AxioVision software on the Nikon Eclipse 80i microscope.

Neutralizing antibody assay

An *in vitro* neutralization assay was performed as previously described.[9,18,19] HEK 293T cells expressing Ad-E4 (84-31 cells) were obtained from the University of Pennsylvania, Department of Genetics, Vector Core, and seeded at 12,000 cells per well in 96-well culture plates. Sera, aqueous humor, and vitreous humor from NHPs were diluted in heat-inactivated fetal bovine serum in a half-log series (1:3.16–1:10,000). Sample dilutions (20 μL) were mixed with 10 μL of the virus serotype expressing eGFP (AAV.CBA.eGFP) and incubated at 37°C for 1 h. A vector concentration of 4.5E + 10 vg/mL was used to achieve a multiplicity of infection (MOI) of 10^4 for AAV7m8, while a titer of 4.5E + 11 vg/mL was used to achieve a MOI of 10^5 for AAV8BP2, which was previously determined to yield 80% GFP-positive cells in the absence of neutralizing sera. Post-injection vitreous titers were compared with baseline anterior chamber fluid titers.

After 48 h, plates were imaged quantitatively for GFP using a Typhoon 9400 Variable Mode Imager (GE Healthcare) with a 520BP40 emission filter and a 488 excitation filter, with the photomultiplier set at 570 V, the sensitivity set at medium, and the focal plane to +3 mm. Images were analyzed for densitometry using ImageJ[20] and the Protein Array Analyzer plugin. Wells were normalized to negative controls lacking virus, and wells with virus but no test sera were averaged and considered 100% GFP. Neutralizing antibody titers are reported as the weakest dilution at which <50% maximal intensity was observed. Samples were run in triplicate and discordant results are reported as the mode.

RESULTS

Transduction of AAV serotypes in the NHP retina

To study the cellular specificity of the two different AAV serotypes in the monkey retina, adult normal-sighted NHPs were selected in order to understand AAV tropism in the adult primate eye. Delivery was carried out using surgical techniques similar to those that would be used in human eyes. AAVs carrying the *eGFP* cDNA driven by a constitutive promoter (Fig. 1a) were injected across a dose range of 1E + 9 vg to 1E + 12 vg in different eyes subretinally and intravitreally (see Tables 1 and 2 and Supplementary Fig. S1; Supplementary Data are available online at www.liebertpub.com/hum). eGFP fluorescence was used to evaluate transduction of the AAV serotypes. Histologic results from retinas and anterior segments of animals injected with AAV7m8 are shown in Figs. 1 and 2, and those from animals injected with AAV8BP2 are shown in Figs. 3–5. There were no complications, and there was no inflammation detected by ophthalmoscopy at any post-injection time point. One animal (animal 9820) injected with AAV7m8 at 1E + 12 vg by IVI had some pain and light sensitivity 1 day post injection. The animal was treated with meloxicam that day for analgesia, and the discomfort resolved. Animals maintained normal activity, food intake and weight, and showed no changes in other clinical parameters. There was no eGFP fluorescence detectable by ophthalmoscopy at early post-injection time points. eGFP was detectable in the original subretinal injection locations in animals that had been injected subretinally starting around 7–14 days after injection, and this was maintained through the last examination.

AAV7m8 transduces the neural retina and anterior segment structures

Histologic evaluations of eGFP-positive cells by direct fluorescence revealed that subretinal injections of AAV7m8 at a dose of 1E + 10 vg resulted in efficient transduction of the RPE and rod photoreceptors (comprising the outer nuclear layer [ONL] and outer and inner segments [OS/IS]), while very few cones were transduced (Fig. 1b and c). The retinal ganglion cells and the axons within the optic nerve were also transduced (Fig. 1d), presumably through exposure of retinal ganglion cells to AAV that refluxed into the vitreous through the retinotomy site. At higher doses (1E + 11 vg and 1E + 12 vg), the cones were efficiently transduced, as seen by co-localization of eGFP with PNA (Fig. 1f and i), and eGFP was produced in more bipolar cells (but no amacrine cells) at 1E + 12 vg (Fig. 1e and h and Supplementary Fig. S2a, b, and d). There was generally more widespread transduction of the optic nerve (Fig. 1g and j) at higher doses, with the parafoveal ganglion cells also transduced (Fig. 1k).

After IVI of AAV7m8, eGFP expression was limited to the ganglion cells, a few bipolar cells, a few Muller glial cells, and the optic nerve at a dose of 1E + 10 vg (Fig. 2a and b). At this dose, the photoreceptors were not transduced, and eGFP

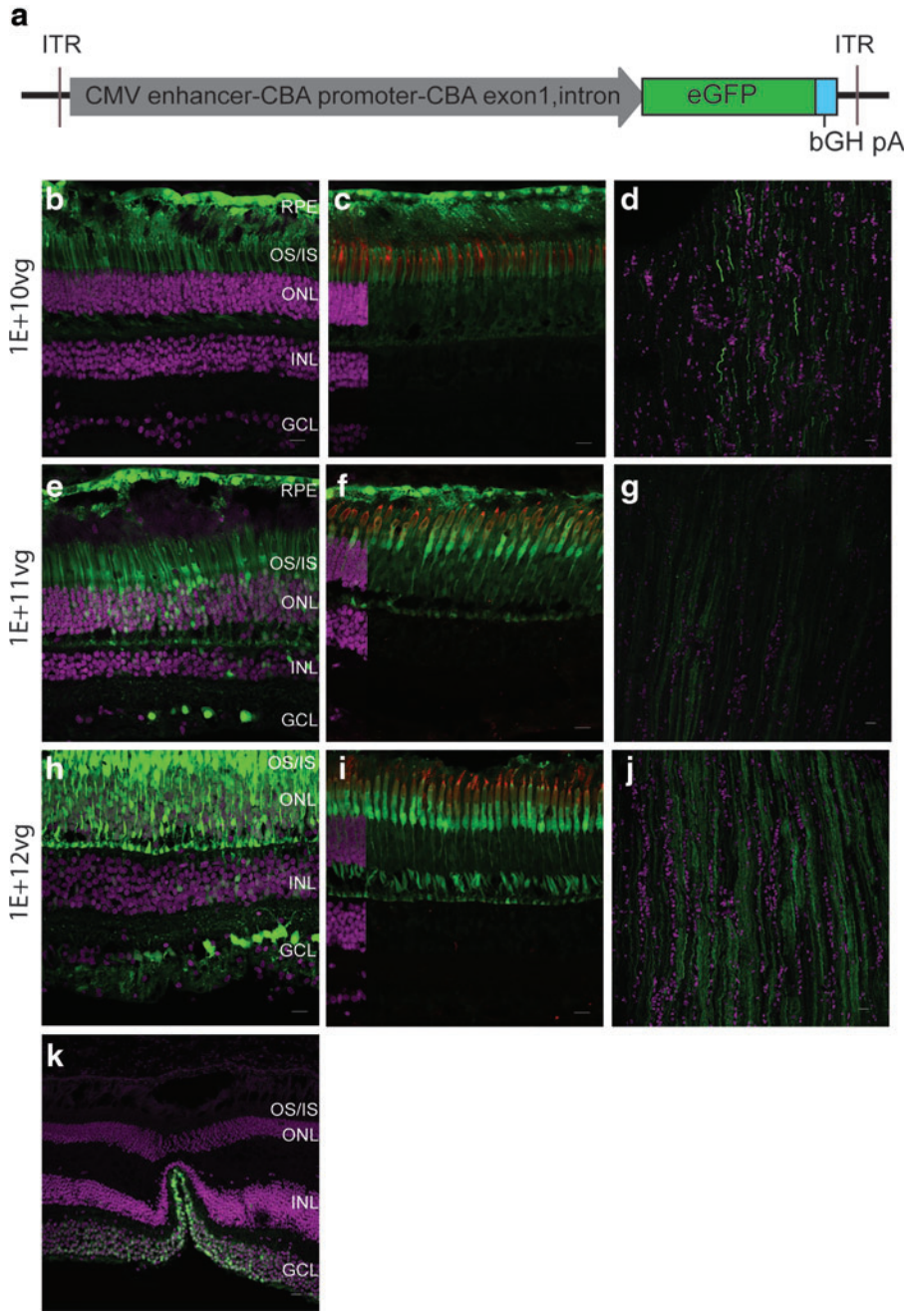

Figure 1. AAV7m8 targets the non-human primate (NHP) outer and inner retina efficiently by subretinal delivery. A cartoon of the adeno-associated virus (AAV) vector is shown comprising a hybrid CMV enhancer-CBA promoter driving *eGFP* expression **(a)**. Confocal images of retinal sections expressing eGFP (*green*) post injection with various doses of AAV7m8-CMV/CBA-eGFP: 1E + 10 vg **(b**, **c**, and **d)**, 1E + 11 vg **(e**, **f**, and **g)**, and 1E + 12 vg **(h**, **i**, and **j)**. Co-localization of eGFP with PNA (*red*), a marker of cone cells, in shown in **(c)**, **(f)**, and **(i)**. The fovea is represented in **(k)** with eGFP expressed in the ganglion cells. DAPI stained nuclei are shown in *magenta*. An overlay of DAPI-stained sections is included on the far left of panels **(c)**, **(f)**, and **(i)** in order to indicate the cell layers. The layer including DAPI fluorescence is eliminated from the remainder of those panels, as it obscures eGFP-positive cells in the nuclear layers. OS/IS, outer segment, inner segment; ONL, outer nuclear layer; INL, inner nuclear layer, GCL, ganglion cell layer. Scale bars represent 50 μm. Color images available online at www.liebertpub.com/hum

was observed in the foveal ganglion cells (Fig. 2c). Lower IVI doses (1E + 8 vg and 1E + 9 vg) did not result in eGFP expression. Efficient photoreceptor transduction was also not observed at a dose of 1E + 11 vg or 6.6E + 11 vg. eGFP expression was limited to retinal ganglion cells, a few bipolar cells, and optic-nerve fibers (Fig. 2d and e). IVI at a higher dose (1E + 12 vg) resulted in eGFP expression in all cell layers of the retina, the RPE, as well as the optic nerve (Fig. 2f–h and Supplementary Fig. S2c).

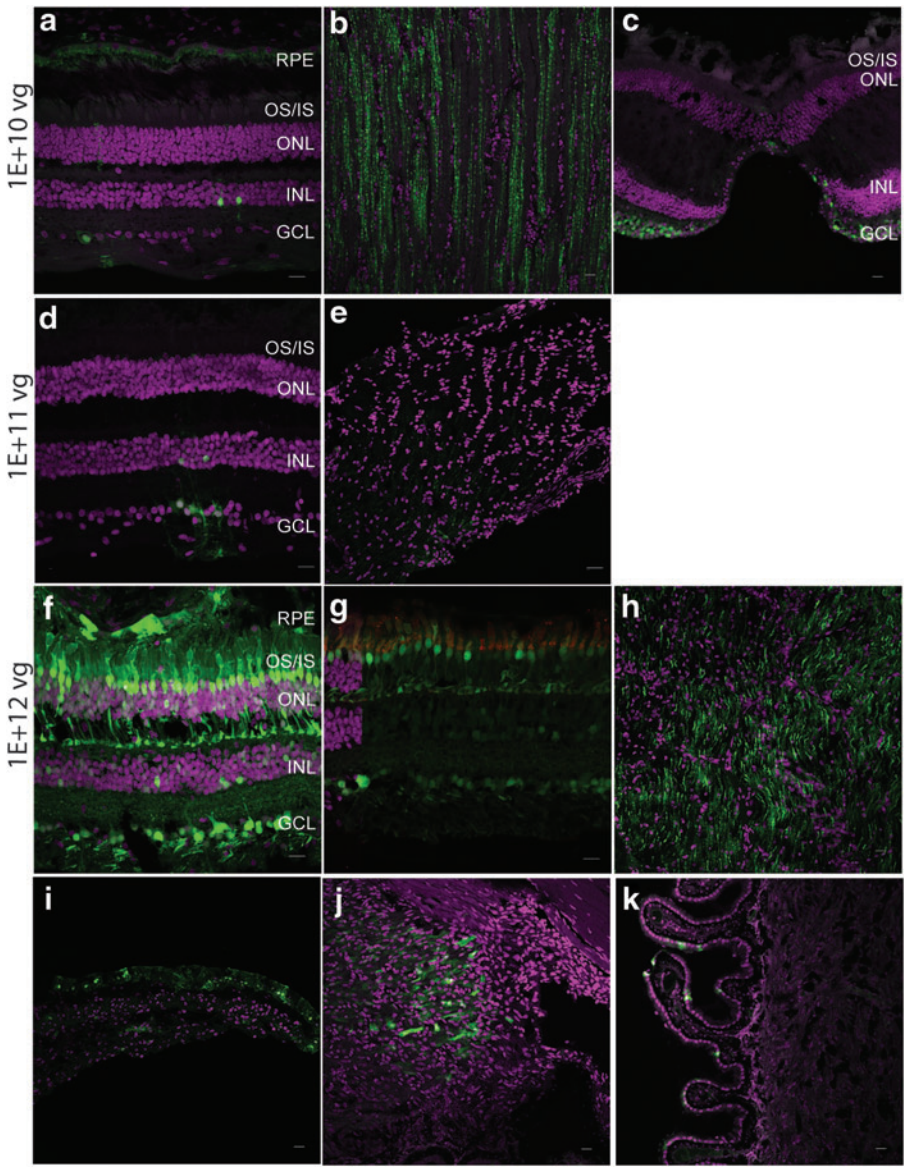

Figure 2. Intravitreal injections (IVI) of AAV7m8 do not target the photoreceptors at lower doses. Confocal images of retina and optic nerve sections after IVI with different doses of AAV7m8. At lower doses of 1E + 10 vg **(a** and **b)** and 1E + 11 vg **(c**, **d**, and **e)**, cells of the INL, GCL, and axons of the optic nerve **(b** and **e)** are transduced. The tissue in panel **(e)** was oriented perpendicular to that shown in **(b)** and **(h)**. At a dose of 1E + 12 vg **(f**, **g**, and **h)**, *eGFP* expression was observed in the photoreceptors and cells of the INL and GCL. eGFP is seen in cone outer segments **(g)** with co-localization of eGFP (*green*) with PNA (*red*). There was expression in retinal ganglion cells emanating from the fovea **(c)**. Sections through the anterior segment reveal transduction of the iris pigmented epithelium **(i)**, the ciliary body **(j)**, and ciliary processes **(k)**. eGFP fluorescence is seen in *green* and DAPI stained nuclei are shown in *magenta*. Scale bars represent 50 μm. Color images available online at www.liebertpub.com/hum

Expression in the amacrine cells was not observed (Supplementary Fig. S2e).

By IVI at doses >1E + 10 vg, the anterior segment structures—the pigmented epithelium of the iris and non-pigmented epithelium of the ciliary body and ciliary processes—were transduced (Fig. 2i–k), while the lens and cornea were not transduced. Subsequently, transduction of the non-pigmented epithelium of the ciliary processes was observed after IVI of AAV7m8 in the wildtype mouse eye (Supplementary Fig. S3a and b).

AAV8BP2 transduces the cone photoreceptors but does not efficiently transduce the bipolar cells in the NHP retina

Subretinal injections of AAV8BP2 at a dose of 1E + 10 vg resulted in eGFP expression in the RPE, photoreceptor cells (in particular the cones), and ganglion cells in the optic nerve (Fig. 3a–c). At higher doses of 1E + 11 vg and 1E + 12 vg, the RPE, photoreceptors, and a few bipolar cells were transduced, in addition to the optic-nerve fibers (Fig. 3d–i). Cone cells were transduced very efficiently at all

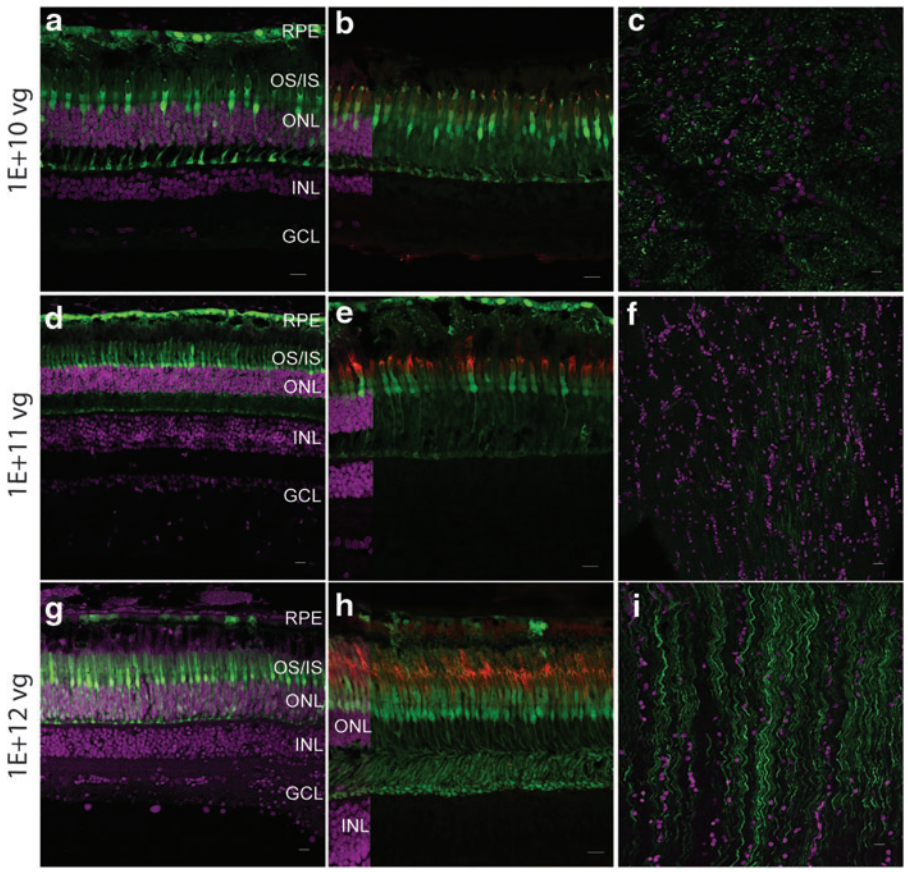

Figure 3. AAV8BP2 transduces photoreceptors efficiently in the primate retina by subretinal delivery. At all three doses 1E + 10 vg **(a**, **b**, and **c)**, 1E + 11 vg **(d**, **e**, **f)**, and 1E + 12 vg **(g**, **h**, and **i)**, AAV8BP2 transduced the photoreceptors (in particular the cones), RPE cells, and optic nerve fibers **(c**, **f**, and **i)**. The tissue in panel **(c)** was oriented tangential to that shown in **(f** and **i)**. Co-localization of eGFP in the cone outer segments is seen with PNA staining (*red*) of the cones in the central panel **(b**, **e**, and **h)**. An overlay of DAPI-stained sections is included on the far left of panels **(b)**, **(e)**, and **(h)** in order to indicate the cell layers. Very few bipolar cells were weakly eGFP positive. eGFP fluorescence is seen in *green*, and DAPI stained nuclei are shown in *magenta*. Scale bars represent 50 μm. Color images available online at www.liebertpub.com/hum

doses injected (Fig. 3b, e, and h). Unlike what was observed in the wildtype mouse,[15] AAV8BP2 did not efficiently transduce the bipolar cells in the NHP retina, and only at the higher doses were (very few) transduced cells observed.

These results prompted the question of whether healthy photoreceptors, as found in the NHP, might form a barrier preventing access of AAV8BP2 to bipolar cells after subretinal injection. Although AAV8BP2 is able to target bipolar cells in mice,[15] since the retina of the mouse is so much thinner than that of large animals and humans, it may be easier for AAV to penetrate the barriers in the mouse than in a large animal retina. Thus, results in mice might not be predictive of results of human clinical trials Therefore, an additional study was carried out, injecting AAV8BP2 subretinally and unilaterally with a vector-expressing eGFP from a bipolar specific 4XmGrm6-SV40 promoter[13] in the eye of a large animal model: a 5-year-old cone-rod dystrophy 1 (crd1) dog. This animal, homozygous for N803del Pde6β mutations, had been shown to have advanced retinal degeneration by optical coherence tomography (OCT) imaging in comparison with a normal-sighted dog around 5 years of age (Fig. 4a and b). By OCT imaging, it was observed that the crd1 dog retina possessed focal areas with increased outer nuclear layer thickness (Fig. 4a and b, middle and bottom rows). By histology, eGFP expression was observed in the ON-bipolar cells (as well as RPE cells, retinal ganglion cells, and optic nerve fibers; Fig. 4c and d). There were higher levels of inner nuclear cell (i.e., bipolar cell) transduction in regions where the photoreceptors had died (Fig. 4c and d), while in "thicker" regions of the retina with more photoreceptor nuclei, there were fewer cells transduced (Fig. 4e). Thus, the photoreceptor cell layer appeared to present a physical barrier to transduction of ON-bipolar cells.

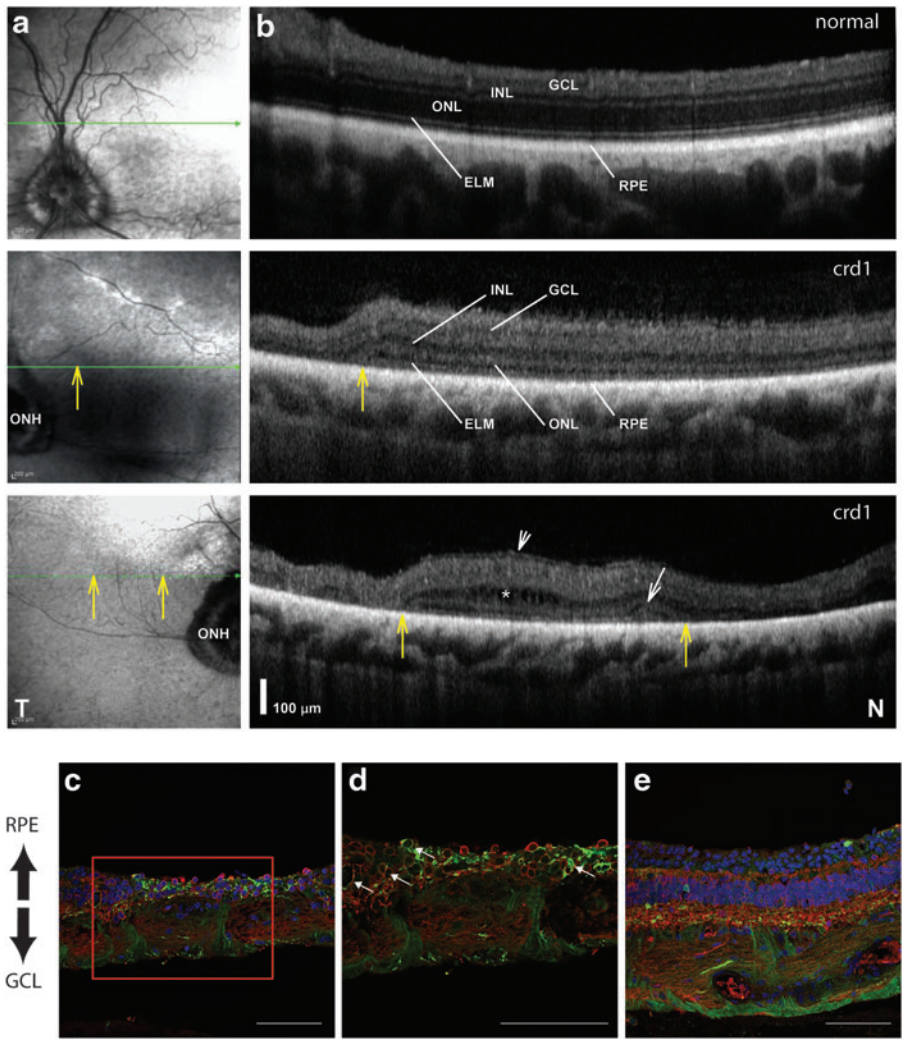

Figure 4. Retinal abnormalities and ON-bipolar transduction with AAV8BP2 in a retinal degeneration dog model. **(a** and **b)** Representative near infrared reflectance (NIR-REF) en-face images (column **a**) and horizontal 9-mm-long spectral domain optical coherence tomography (SD-OCT; column **b**) cross-sections in a representative normal dog around 5 years old (*top row*) compared with images from the retina nasal (*middle row*) and temporal (*bottom row*) to the optic nerve head (ONH) of a 5-year-old *crd1* dog. This crd1 dog was injected subretinally in the temporal retina with AAV8BP2-4XGrm6-CatCh-eGFP at a titer of 1E + 11 vg. SD-OCT scans covered approximately 18 mm of retina along a horizontal line crossing just above the ONH (*thin green arrow* in column **a**) along the boundary between tapetal and non-tapetal retina; shown are 7-mm-long SD-OCT images cropped to match location of the normal and *crd1* dog nasal retinas. The external limiting membrane (ELM) is a thin line that lies just above a hyperreflective retinal pigment epithelium (RPE). *Vertical yellow arrows* point to regions of transitions to hyper-reflective, lighter regions on NIR-REF images, which co-localized with delaminated thinned retina on SD-OCT. Large regions of well-laminated retina nasal to the ONH (*middle row*) shows a thinned ONL in the *crd1* dog (23 μm) compared with that of the normal dog (86 μm; *top row*). The *crd1* eye also shows patchy depigmentation on NIR-REF images (*middle row*, to the *left* of *yellow arrow*) co-localizing with severe retinal thinning, particularly around the ONH. Photoreceptor degeneration is associated with a relatively thickened inner retina (*middle row*, INL and retina superficial to it) with epiretinal membrane formation at the surface (*bottom row, short diagonal arrow*) and intraretinal hypo-reflective images (*asterisk*) that suggest intraretinal edema. At the transition zone, there can be an elevation of the ELM just before approximating the RPE in areas of transition to total photoreceptor (ONL) loss resembling a stage of outer retinal tubulation (*white diagonal arrow*). T, temporal; N, nasal retina. Histologic sections **(c–e)** of the *crd1* temporal retina reveals eGFP (*green*) 1 month post injection. In **(c)**, co-localization of eGFP with ON-bipolar cells was confirmed with immunohistochemistry using anti-Goα antibodies (*red*). The *boxed* region in **(c)** is magnified in **(d)** with *arrows* indicating transduced ON-bipolar cells in regions of retinal thinning. Panel **(e)** is a region of thicker retina with more outer nuclei with eGFP (*green*), ON-bipolar cells (*red*) and nuclei (*blue*) labeled. Scale bars represent 50 μm. Color images available online at www.liebertpub.com/hum

By the intravitreal route, AAV8BP2 at a dose of 1E + 10 vg did not transduce the NHP retina or optic nerve. At 1E + 11 vg, eGFP expression was observed in the ganglion cells and the optic nerve (Fig. 5a and b). At a higher dose of 1E + 12 vg, the ganglion cells and optic nerve produced eGFP (Fig. 5c and d). A few bipolar cells were also eGFP positive at 1E + 11 and 1E + 12 vg. The foveal ganglion cells were also transduced at 1E + 12 vg (Fig. 5e). In addition, eGFP was observed in the

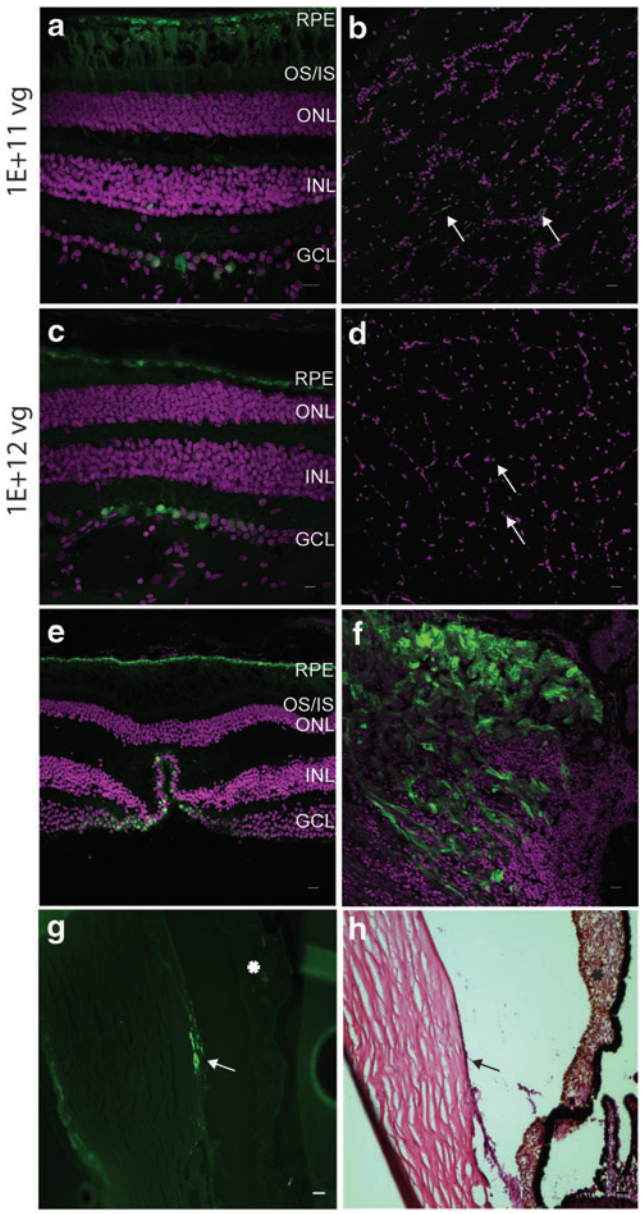

Figure 5. AAV8BP2 targets the ganglion cells by intravitreal delivery. *eGFP* expression at different viral titers: 1E + 11 vg **(a** and **b)** and 1E + 12 vg **(c** and **d)** post injection with AAV8BP2. IVI led to expression in the ganglion cell axons in the optic nerve **(b** and **d)**, foveal ganglion cells **(e)**, ciliary body **(f)**, and cornea (*arrow*, **g**). **(h)** is a hematoxylin and eosin–stained section of the corneal region shown transduced in (**g**; *arrow*). The *asterisk* indicates the iris in **(g)** and **(h)**. eGFP fluorescence is seen in *green*, and DAPI-stained nuclei are shown in *magenta*. Scale bars represent 50 μm. Color images available online at www.liebertpub.com/hum

cells of the ciliary body and cornea at 1E + 12 vg (Fig. 5f and g), although no other anterior structures (the iris or lens) were transduced.

In summary, both AAV7m8 and AAV8BP2 are capable of transducing a variety of retinal cell types (Table 2) after IVI and subretinal injection, and as expected for each vector, there are increased numbers of transduced cells as the dose is increased. Although AAV8BP2 was generated by selecting for an AAV that would target mouse bipolar cells, it did not target wildtype NHP bipolar cells efficiently. This may be because of the thicker tissue barriers in large animal retinas, as supported by results in the degenerating retina of a dog model of retinitis pigmentosa. Finally, both AAV7m8 and 8P2 transduced cells in the anterior segment after high-dose IVI.

eGFP expression in the optic pathway

Brain tissue was evaluated for the presence of eGFP in NHPs that were injected with AAV7m8 by IVI and subretinal injections at 1E + 12 vg. eGFP expression was observed in the nerve fibers of the optic tract by subretinal and IVI routes and the lateral geniculate nucleus (LGN; Fig. 6a–e). In the LGN, eGFP was observed terminating only in layers 1 and 2, which receive input from the magnocellular-projecting (M) ganglion cells of the retina (also known as alpha or parasol ganglion cells). eGFP was not observed in other cells in the brain, including the visual cortex, indicating that there was no trans-synaptic transmission from the LGN with AAV7m8.

When AAV8BP2-injected monkey brain sections were analyzed to look for transduction of the optic pathway, eGFP was observed in the nerve fibers of the optic tract (Fig. 6f), but no terminations in the LGN were observed, even at the highest dose of 1E + 12 vg.

Immune reactivity to AAV7m8 and AAV8BP2

Anti-AAV neutralizing antibodies were assayed in the serum and in the ocular fluid collected at baseline (pre-injection) and 1 month post injection at the time of euthanasia (Table 3).

In general, the baseline titer in the serum and ocular fluid was found to be low (<1:10), except in one animal (07D179M) where the baseline titer was 1:100. This particular animal was injected with AAV7m8 by IVI at a dose of 1E + 9 vg. eGFP expression was not observed in this animal retina, suggesting that either the low dose or the high baseline titer contributed to the lack of eGFP expression observed. In the serum, varying increases in neutralizing antibody titers were observed at different doses of AAV7m8, the highest being 1:1,000. In addition, IVI of AAV7m8 at the highest dose of 1E + 12 vg led to an increase in the neutralizing antibody titer from baseline in the anterior chamber fluid and vitreous (Table 3).

AAV8BP2 had lower neutralizing antibody titers post injection in the vitreous and anterior chamber fluid compared with AAV7m8, even at the

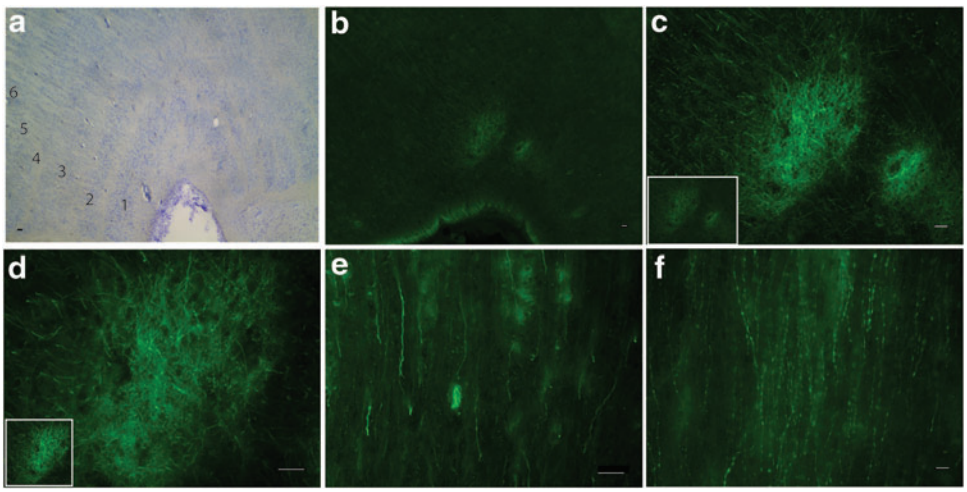

Figure 6. Transduction in the nerve fibers of the visual pathway. Images of horizontal sections of the lateral geniculate nucleus (LGN) of the NHP brain after IVI of AAV7m8 **(a–d)**. Nissl staining illustrating the various (1–6) LGN layers **(a)**. eGFP expression (*green*) is seen in layers 1 and 2 of the LGN **(b)**, and further magnification (of the image in the *inset*) indicates expression in the nerve fibers **(c** and **d)**. The optic tract also contained eGFP positive nerve fibers **(e)**. AAV8BP2-injected animals had eGFP in the nerve fibers of the optic tract **(f)**. Scale bars represent 50 μm. Color images available online at www.liebertpub.com/hum

highest titers. AAV8BP2 did induce a high neutralizing antibody response in the serum by IVI at doses of 1E + 11 and 1E + 12 vg, while the antibody titers were lower after subretinal injections at the same titers (Table 3).

Histopathologic findings after intraocular injection of AAV7m8 or AAV8BP2

This study looked at the presence of glial fibrillary acidic protein (GFAP) as a marker of glial activation in the transduced retinas with AAV7m8 and AAV8BP2 at the highest doses (1E + 11 and 1E + 12 vg). Normally, in wildtype, untreated retinas, GFAP is restricted to the end feet of the Muller glial cells in the inner retina, while during degeneration or retinal detachment, GFAP expression increases and is observed throughout the Muller cell processes.[21] Subretinal injections of AAV8BP2 at a dose of 1E + 11 vg showed GFAP-positive processes mostly at the Muller cell end feet, with some positive processes extending into the ONL, while IVI at the same dose seemed to lead to lower GFAP immunoreactivity (Supplementary Fig. S4a and c). At 1E + 12 vg (AAV8BP2 subretinal and IVI), GFAP activation was greater and extended to fill the width of the retina (Supplementary Fig. S4b and d). High GFAP immunoreactivity was observed at doses of 1E + 12 vg when AAV7m8 was delivered

Table 3. *Neutralizing antibody (Nab) titers in the serum and ocular fluid*

AAV serotype	*NHP ID*	*Delivery route*	*Dose (vg)*	*Baseline serum titer*	*Post-injection serum titer*	*Baseline AC*	*Post-injection AC*	*Post-injection vitreous*
AAV8b	05D 370 M	IVI	1E + 09	1: 3.16	1: 31.6	<1:3.16	<1:3.16	<1:3.16
	05C 028	IVI	1E + 10	<1:3.16	1: 10	<1:3.16	<1:3.16	<1:3.16
	9986	IVI	1E + 11	<1:3.16	1:100	<1:3.16	<1:3.16	<1:3.16
	9986	IVI	1E + 12	<1:3.16	1:100	<1:3.16	<1:3.16	<1:3.16
	04C 094 F	SR	1.0E + 10	<1:3.16	1:31.6	<1:3.16	<1:3.16	<1:3.16
	04C 076 F	SR	1.5E + 11	<1:3.16	<1:3.16	<1:3.16	<1:3.16	<1:3.16
	99-09 F	SR	1E + 12	<1:3.16	1:10	<1:3.16	<1:3.16	<1:3.16
AAV7m8	05C 068 M	IVI	1E + 08	<1:3.16	1 : 316	<1:3.16	<1:3.16	1 : 3.16
	07D 179 M	IVI	1E + 09	1 : 100	1 : 316	<1:3.16	<1:3.16	<1:3.16
	05C 028	IVI	1E + 10	<1:3.16	1 : 10	<1:3.16	<1:3.16	<1:3.16
	5098	IVI	1E + 11	1:10	1:1000	<1:3.16	1:3.16	<1:3.16
	9820	IVI	6.67E + 11	1:3.16	1:10	<1:3.16	1:3.16	1:100
	9820	IVI	1E + 12	1:3.16	1:10	<1:3.16	1:10	1:100
	04C 094 F	SR	1.0E + 10	<1:3.16	1:100	<1:3.16	1:3.16	<1:3.16
	9817	SR	5.33E + 10	1:3.16	1:10	<1:3.16	<1:3.16	1:3.16
	04C 076 F	SR	1.5E + 11	<1:3.16	1 :10	<1:3.16	<1:3.16	<1:3.16
	5285	SR	1E + 12	<1:3.16	1: 31.6	<1:3.16	<1:3.16	<1:3.16

subretinally or intravitreally with GFAP-positive processes extending throughout the retina, while at 1E + 11 vg, GFAP expression was mostly limited to the Muller cell end feet (Supplementary Fig. S4e–h).

The health of the retinas was assessed by histopathological analysis of H&E-stained sections. AAV7m8 injected either subretinally or intravitreally at doses of 1E + 10 and 1E + 11 vg did not result in the presence of any inflammatory cells (Supplementary Fig. S5a, b, d, and e). However, severe chronic inflammation was observed at 1E + 12 vg after subretinal injection of AAV7m8. There were lymphocytic infiltrates in all layers of the retina, perivascular inflammation in the retina, loss of RPE (Supplementary Fig. S5f), and chronic choroidal inflammation (Supplementary Fig. S5g). High-dose IVI of AAV7m8 (1E + 12 vg) also resulted in retinal infiltrates but no choroidal inflammation (Supplementary Fig. S5c).

AAV8BP2 at doses of 1E + 11 vg by either route of delivery did not cause inflammation, and the retinas had normal morphology (Supplementary Fig. S5h and j). In contrast to AAV7m8, the highest dose of AAV8BP2 (1E + 12 vg) did not cause choroidal or perivascular inflammation or loss of RPE, but retinal infiltrates were observed at the nerve fiber layers after subretinal injection (but not by IVI; Supplementary Fig. S5j and k).

In summary, these studies show that there were subclinical signs of inflammation (elevated GFAP expression and retinal infiltrates) after injection with the highest dose (1E + 12 vg) of either serotype. AAV7m8 also induced chronic inflammation after subretinal injection.

DISCUSSION

Recent results of human gene therapy clinical trials targeting a form of early onset blindness have bolstered interest in applying retinal gene therapy to other genetic and acquired conditions causing vision loss.[22] There are now a variety of data showing the safety of intraocular delivery of AAV2 at least up to doses of 1.5E + 11 vg,[1,2,22] and although the capacity of AAV is small, many of the retinal disease genes fit into AAV. Thus, there are many different retinal gene therapy strategies in the pipeline, including gene augmentation, knockdown, gene editing, delivery of neurotrophic factors, and delivery of reagents, which modulate pathways controlling oxidative stress, neovascularization, or metabolism.[23–27] In addition, there has been an expansion of the "vector toolkit," with the goal of enhancing and facilitating delivery of gene-based treatments to the appropriate cell types and through different delivery routes.[28–32] Proof-of-concept studies in mouse models have shown that some of these vectors can be used to treat different inherited retinal degenerative diseases using gene augmentation or optogenetic strategies and through different routes of delivery.[10–15] Because of the many anatomic, biologic, and physiologic differences between the retinas of mouse and man and the related differences in surgical access between the two species, this study characterized the cellular targets and safety of two novel AAVs generated by evolutionary design in the eye of an animal model most similar to that of humans: the NHP. This study shows that one cannot extrapolate directly between mice and "men."

One of the features that made AAV7m8 so intriguing in the mouse was that in addition to targeting ganglion cells, it could penetrate to photoreceptors and RPE cells in the outer retina after injection into the vitreous.[10,12] We found in NHPs that IVI of AAV7m8 transduced photoreceptors and RPE efficiently only at the highest dose of 1E + 12 vg. Severe inflammation was also observed at this dose, along with indications of permanent neuronal cell injury (GFAP immunoreactivity) and development of high neutralizing antibody titers. The extent of ganglion cell transduction from eye to eye after injection of AAV7m8 was likely dependent on the location of the injection with respect to the ganglion cell–enriched macula.

The features of AAV8BP2 that made it particularly interesting after studies in the mouse were that it targeted cone photoreceptors and bipolar cells efficiently after subretinal injection and ganglion cells after IVI.[15] Although cone photoreceptors were transduced efficiently after subretinal injection of AAV8BP2 in the NHP, very few bipolar cells were transduced, even at the highest doses. AAV8BP2 targeted few retinal ganglion cells after either subretinal or intravitreal delivery in the NHP.

The lack of penetration through or across the NHP retina of both AAV7m8 and AAV8BP2 may simply relate to the increased thickness of the NHP retina compared with the mouse retina. Disease conditions that destroy cell layers may enhance protein trafficking where it is normally absent. To test this possibility, AAV8BP2 was delivered subretinally using a bipolar specific promoter in a retinal degeneration large animal model. eGFP expression was observed in the ON-bipolar cells in regions with extensive degeneration (but not in adjacent thicker retina), suggesting that remaining retinal photoreceptors present a physical barrier to

transduction of ON-bipolar cells. Thus, it is possible that AAV8BP2 could be used to target the inner retina of humans if the photoreceptor layer has been compromised, as it is in retinal and macular degenerative conditions. Unfortunately, there is no NHP model with which to explore this possibility further.

Results from the NHP experiments also revealed that AAV7m8 and AAV8BP2 can transduce anterior segment structures in addition to retinal cells. AAV7m8 targeted the epithelium of the iris and ciliary processes, and AAV8BP2 targeted the ciliary body and cornea in the NHP eye. Thus, AAV8BP2 may have potential therapeutic applications for modulation of intraocular pressure in diseases such as glaucoma due to transduction of the anterior chamber structures. In addition, ciliary body transduction may be useful for delivering stable supplies of diffusible molecules that could be used to treat a variety of different diseases, including wet AMD, and AAV7m8 could be useful in strategies involving diffusible agents such as neurotrophic factors, antioxidants, nutrients, antibodies, or even compounds that could modulate intraocular pressure.[23–26] Transduction of these structures, however, could also have an impact on safety. It is possible that transduction of anterior segment structures is partially responsible for immunologic/inflammatory sequelae that were apparent after high-dose IVI of AAV7m8. AAV8BP2 had a better safety profile than AAV7m8 did with respect to retina inflammation, even at the highest dose of 1E + 12 vg, and according to whether subretinal or intravitreal delivery was used.

Taken together, these data show that studies in rodents may not provide sufficient information for understanding the cellular transduction and pharmacologic properties of engineered AAVs, and thus for considering the risks and benefits of moving forward with a particular AAV capsid for translational studies. This study was designed to use the minimum number of "recycled" NHPs/eyes, and so does not provide data relating to consistency of transduction and immunological findings for particular AAVs/doses. Further, since NHPs were born in the wild and are outbred, there will be variability in response similar to what one might expect in humans. However, the trend of responses according to vector and dose reveal the outcomes one would predict for safety and cellular specificity of transduction in humans and thus provide guidelines for formal preclinical toxicity studies.

ACKNOWLEDGMENTS

We are grateful to Jolaine M. Wilson, DVM, for assistance with animal procedures and to the Shindler Lab for assistance with histopathology staining procedures. We were supported by the Foundation Fighting Blindness-sponsored CHOP-Penn Pediatric Center for Retinal Degenerations, National Eye Institute/NIH grants R21EY020662 and 8DP1EY023177, Research to Prevent Blindness, the Paul and Evanina Mackall Foundation Trust, the Center for Advanced Retinal and Ocular Therapeutics, and the F.M. Kirby Foundation.

AUTHOR DISCLOSURE

Drs. Maguire and Bennett are co-inventors on a patent for "a method of treating or retarding the development of blindness" (US Patent No. 8,147,823) but waived any potential financial interest in this technology in 2002.

Dr. Bennett is a founder of Gensight Biologics and a scientific (non-equity-holding) founder of Spark Therapeutics. Drs. Bennett and Cronin are co-authors of a provisional patent describing properties of the AAV capsid 8BP2.

The other authors declare that they have no conflicts of interest.

REFERENCES

1. Testa F, Maguire AM, Rossi S, et al. Three-year follow-up after unilateral subretinal delivery of adeno-associated virus in patients with Leber congenital Amaurosis type 2. Ophthalmology 2013; 120:1283–1291.
2. Bennett J, Ashtari M, Wellman J, et al. AAV2 gene therapy readministration in three adults with congenital blindness. Sci Transl Med 2012; 4: 120ra115.
3. Bennett J, Wellman J, Marshall KA, et al. Safety and durability of effect of contralateral-eye administration of AAV2 gene therapy in patients with childhood-onset blindness caused by RPE65 mutations: a follow-on Phase 1 trial. Lancet 2016;388:661–672.
4. Grimm D, Zolotukhin S. E Pluribus Unum: 50 years of research, millions of viruses, and one goal – Tailored acceleration of AAV evolution. Mol Ther 2015;23:1819–1831.
5. Santiago-Ortiz J, Ojala DS, Westesson O, et al. AAV ancestral reconstruction library enables selection of broadly infectious viral variants. Gene Ther 2015;22:934–946.
6. Yin L, Greenberg K, Hunter JJ, et al. Intravitreal injection of AAV2 transduces macaque inner retina. Invest Ophthalmol Vis Sci 2011;52:2775–2783.
7. Dalkara D, Kolstad KD, Caporale N, et al. Inner limiting membrane barriers to AAV-mediated retinal transduction from the vitreous. Mol Ther 2009;17:2096–2102.
8. Tolmachova T, Tolmachov OE, Barnard AR, et al. Functional expression of Rab escort protein 1 following AAV2-mediated gene delivery in the

retina of choroideremia mice and human cells *ex vivo*. J Mol Med 2013;91:825–837.

9. Bennicelli J, Wright JF, Komaromy A, et al. Reversal of blindness in animal models of leber congenital amaurosis using optimized AAV2-mediated gene transfer. Mol Ther 2008;16:458–465.
10. Dalkara D, Byrne LC, Klimczak RR, et al. *In vivo*-directed evolution of a new adeno-associated virus for therapeutic outer retinal gene delivery from the vitreous. Sci Transl Med 2013;5: 189ra176.
11. Gaub BM, Berry MH, Holt AE, et al. Restoration of visual function by expression of a light-gated mammalian ion channel in retinal ganglion cells or ON-bipolar cells. Proc Natl Acad Sci U S A 2014;111:E5574–5583.
12. Mace E, Caplette R, Marre O, et al. Targeting channelrhodopsin-2 to ON-bipolar cells with vitreally administered AAV Restores ON and OFF visual responses in blind mice. Mol Ther 2015;23:7–16.
13. Lagali PS, Balya D, Awatramani GB, et al. Light-activated channels targeted to ON bipolar cells restore visual function in retinal degeneration. Nat Neurosci 2008;11:667–675.
14. Scalabrino ML, Boye SL, Fransen KM, et al. Intravitreal delivery of a novel AAV vector targets ON bipolar cells and restores visual function in a mouse model of complete congenital stationary night blindness. Hum Mol Genet 2015;24:6229–6239.
15. Cronin T, Vandenberghe LH, Hantz P, et al. Efficient transduction and optogenetic stimulation of retinal bipolar cells by a synthetic adeno-associated virus capsid and promoter. EMBO Mol Med 2014;6:1175–1190.
16. Stieger K, Colle MA, Dubreil L, et al. Subretinal delivery of recombinant AAV serotype 8 vector in dogs results in gene transfer to neurons in the brain. Mol Ther 2008;16:916–923.
17. Liu X, Yan Z, Luo M, et al. Species-specific differences in mouse and human airway epithelial biology of recombinant adeno-associated virus transduction. Am J Respir Cell Mol Biol 2006;34: 56–64.
18. Vandenberghe LH, Bell P, Maguire AM, et al. Dosage thresholds for AAV2 and AAV8 photoreceptor gene therapy in monkey. Sci Transl Med 2011;3:88ra54.
19. Amado D, Mingozzi F, Hui D, et al. Safety and efficacy of subretinal readministration of a viral vector in large animals to treat congenital blindness. Sci Transl Med 2010;2:21ra16.
20. Schindelin J, Arganda-Carreras I, Frise E, et al. Fiji: an open-source platform for biological-image analysis. Nat Methods 2012;9:676–682.
21. Hippert C, Graca AB, Barber AC, et al. Muller glia activation in response to inherited retinal degeneration is highly varied and disease-specific. PLOS ONE 2015;10:e0120415.
22. MacLaren RE, Bennett J, Schwartz SD. Gene therapy and stem cell transplantation in retinal disease: the new frontier. Ophthalmology 2016; 123:S98–S106.
23. Borras T, Elliott R, Buie L, et al. Transgene targeting of the iris pigment epithelium (IPE) to study and potentially treat pseudoexfoliation glaucoma. Invest Ophthalmol Vis Sci 2014;55: 5667–5667.
24. Hou XR, Miao H, Tao Y, et al. Expression of cytokines on the iris of patients with neovascular glaucoma. Acta Ophthalmol 2015;93:e100–104.
25. El Sanharawi M, Touchard E, Benard R, et al. Long-term efficacy of ciliary muscle gene transfer of three sFlt-1 variants in a rat model of laser-induced choroidal neovascularization. Gene Ther 2013;20:1093–1103.
26. Grimm D, Zhou S, Nakai H, et al. Preclinical *in vivo* evaluation of pseudotyped adeno-associated virus vectors for liver gene therapy. Blood 2003;102: 2412–2419.
27. Black A, Vasireddy V, Chung DC, et al. Adeno-associated virus 8-mediated gene therapy for choroideremia: preclinical studies in *in vitro* and *in vivo* models. J Gene Med 2014;16:122–130.
28. Kay CN, Ryals RC, Aslanidi GV, et al. Targeting photoreceptors via intravitreal delivery using novel, capsid-mutated AAV vectors. PLOS ONE 2013;8:e62097.
29. Petrs-Silva H, Dinculescu A, Li Q, et al. High-efficiency transduction of the mouse retina by tyrosine-mutant AAV serotype vectors. Mol Ther 2009;17:463–471.
30. Petrs-Silva H, Dinculescu A, LiQ, et al. Novel properties of tyrosine-mutant AAV2 vectors in the mouse retina. Mol Ther 2011;19:293–301.
31. Mowat FM, Gornik KR, Dinculescu A, et al. Tyrosine capsid-mutant AAV vectors for gene delivery to the canine retina from a subretinal or intravitreal approach. Gene Ther 2014;21:96–105.
32. Vandenberghe LH, Bell P, Maguire AM, et al. AAV9 targets cone photoreceptors in the nonhuman primate retina. PLOS ONE 2013;8:e53463.

Received for publication July 21, 2016;
accepted after revision October 13, 2016.

Published online: October 17, 2016.